

Chondrogenic potential of PMSCs cultured on chondroitin sulfate/gelatin-modified DBM scaffold

Fatemeh Haghwerdi¹, Ismaeil Haririan^{1,2*}, Masoud Soleimani^{3*}

¹Department of Pharmaceutical Biomaterials and Medical Biomaterial Research Center (MBRC), Faculty of Pharmacy, Tehran University of Medical Science, Tehran, Iran

²Department of Pharmaceutics, Faculty of Pharmacy, Tehran University of Medical Sciences, Tehran, Iran

³Department of Hematology, Faculty of Medical Sciences, Tarbiat Modares University, Tehran, Iran

Article Info



Article Type:

Original Article

Article History:

Received: 16 Jul. 2023

Revised: 15 Oct. 2023

Accepted: 15 Oct. 2023

ePublished: 27 Oct. 2024

Keywords:

Demineralized bone matrix, Chondroitin sulfate, Gelatin, PMSCs, Chondrogenic potential

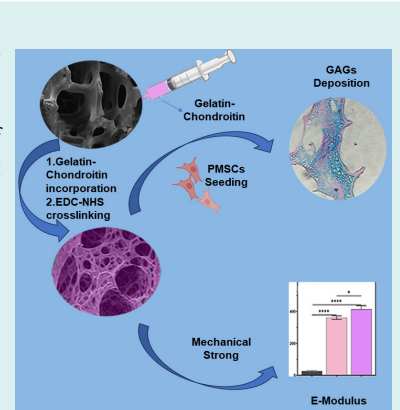
Abstract

Introduction: Osteoarthritis is one of the most common orthopedic diseases that gradually causes wear and damage to the articular Subchondral bone due to the destruction of articular cartilage. One of the basic challenges in cartilage tissue engineering is the choice of scaffold. In the design of the cartilage scaffold, it is useful to consider parameters such as porosity, water absorption, high mechanical resistance, biocompatibility, and biodegradability. Therefore, in this study, demineralized bone matrix (DBM), which inherently has these characteristics to some extent, was chosen as the basic scaffold.

Methods: The gelatin/DBM (G/DBM) and the chondroitin sulfate-gelatin/DBM (GCS/DBM) scaffolds were prepared, respectively, by incorporating gelatin or chondroitin sulfate/gelatin solution inside DBM pores, freeze-drying and crosslinking with EDC/NHS. The physicochemical, biological characteristics and chondrogenic potential of scaffolds were studied.

Results: According to the SEM results, the size of the DBM pores in the G/DBM and GCS/DBM scaffolds decreased (from almost 100-1500 μm to less than 200 μm), which reduced cell escape compared to the DBM scaffold. Also, crosslinking the scaffolds has greatly increased their compressive E-modulus (more than 8 times). The cytocompatibility and non-toxicity of all scaffolds were confirmed by acridine orange/ethidium bromide (AO/EB) staining. The evaluation results of chondrogenic differentiation of placenta-derived mesenchymal stem cells (PMSCs) on modified scaffolds, using the real-time PCR method, showed that the presence of CS in the GCS/DBM scaffold improved the expression of chondrogenesis markers such as Aggrecan (AGC) (~4 times) and collagen 2 (COL-2) (~2.2 times) compared to the DBM scaffold. Also, Alcian blue staining and immunohistochemical analyses of the scaffolds showed denser and more coherent GAGs and COL-2 protein synthesis on the GCS/DBM than the G/DBM and DBM scaffolds.

Conclusion: According to the results, the GCS/DBM scaffold can be a suitable scaffold for cartilage tissue engineering.



Introduction

Articular cartilage tissue inherently has a low self-healing ability due to the inherent characteristics of cartilage cells such as low mitosis rate, low cell number, and lack of blood vessels, inflammatory and nerve cells, which causes weak tissue self-healing ability. Therefore, articular cartilage injuries do not often heal by themselves, and even minor injuries can lead to further destruction of

articular cartilage and osteoarthritis.¹ These lesions affect not only the elderly but also young athletes. Weight-bearing joints such as the knee may develop defects in the articular cartilage due to stress, trauma, injury, or disease, leading to joint pain or locking.² Although this disease is not fatal, it is very common worldwide, both in developed and developing countries, and causes movement problems and disability with severe pain.



*Corresponding authors: Ismaeil Haririan, Email: haririan@tums.ac.ir; Masoud Soleimani, Email: soleim_m@modares.ac.ir



© 2025 The Author(s). This work is published by BioImpacts as an open access article distributed under the terms of the Creative Commons Attribution Non-Commercial License (<http://creativecommons.org/licenses/by-nc/4.0/>). Non-commercial uses of the work are permitted, provided the original work is properly cited.

According to the WHO, osteoarthritis is the most common joint disorder in the United States. In 2020, more than 32.5 million adults were diagnosed with arthritis. Worldwide, more than 22% of adults over 40 have knee osteoarthritis. Out of this number, women are about 62% of the patients.³ Also, according to the reports of the WHO, due to the increase in age and life expectancy in societies, it is predicted that the number of people suffering from this disease will increase by more than 50% in the next 20 years (about half a billion people).^{4,5} Considering the low efficiency of existing treatment methods (such as mosaicplasty, microfracture and autologous cartilage implantation (ACI) and matrix-assisted cartilage implantation (MACI) in repairing damaged cartilage tissue, it seems that cartilage tissue engineering (CTE) can be an approach suitable to overcome this problem.⁶ The choice of the appropriate scaffold greatly influences the efficiency of CTE in cartilage tissue engineering in terms of the similarity in construction materials, three-dimensional and spatial shape, porosity, swelling, biocompatibility, biodegradability, and mechanical properties.^{7,8}

One of the important points of view in tissue engineering is to imitate natural tissue structure in the design of the spatial structure and materials of selected scaffolds.

For the first time in 2013, Liese et al studied the DBM scaffold with chondrocyte-macroaggregates 3-D cells for the regeneration of cartilage tissue, which observed dedifferentiation and apoptosis in chondrocytes.⁹

The studies of Hongjie et al showed that implantation of hybrid scaffolds, consisting of chitosan-glycerol phosphate thermal and DBM or DBM - E7 bioactive peptide, is more successful than the microfracture procedure for repairing damaged cartilage tissue.^{10,11} Due to the biological and inherent characteristics of the demineralized and decellularized matrix of bone tissue (DBM), such as three-dimensionality and porosity, biocompatibility and biodegradability with appropriate mechanical strength and its abundance and availability (unlike the cartilage extracellular matrix, makes it a good choice for cartilage tissue engineering. Therefore, DBM was chosen as the basic scaffold.¹²

Gelatin is a non-cytotoxic, biodegradable, and biocompatible natural polymer with low immunogenicity obtained from the hydrolytic process of collagen. In addition, gelatin contains an arginine-glycine-aspartic acid (RGD) motif that supports cell proliferation, migration, and adhesion.¹³

Chondroitin sulfate (CS) is a glycosaminoglycan (GAG) in the ECM of normal cartilage that protects the structural integrity of cartilage and contributes to the restoration of arthritic joint function via maintaining the niche of stem cells, adjusting enzyme activity and anti-inflammatory activity.¹⁴

This study aimed to design a biocompatible and biodegradable scaffold consisting of biologically active

materials with a microstructure similar to natural cartilage. Therefore, the DBM-based scaffold with physical properties such as biomaterial structure, inherent 3D, porosity, and swelling ability was chosen. The size of DBM pores was optimized by gelatin incorporation to reduce the cell escape. Chemical crosslinking enhances the scaffold's mechanical strength and improves the chondrogenic properties of the scaffold. CS composition, which is one of the basic constituents of the cartilage tissue, was included in the scaffold structure.

The DBM scaffold has high cell escape and low cell adhesion; it is hoped that these problems will be reduced by introducing gelatin solution into the DBM pores. Also, chemical crosslinking can help to increase the stability and mechanical strength of the scaffold, and it is hoped that the chondrogenic potential of the GCS/DBM scaffold will be improved with the help of the presence of CS, which is a component of the extracellular matrix of cartilage tissue.

Materials and Methods

DBM was provided by (Tissue Regeneration Corporation, Kish, Iran). CS was purchased from (Karen Pharma and Food Supplement CO., Yazd, Iran). Gelatin type A, -Ethyl-3-(3-dimethylaminopropyl) carbodiimide (EDC), and N-Hydroxy succinimide (NHS) were provided from (Sigma, Taufkirchen, Germany).⁴,6-diamidino-2-phenylindole (DAPI), DMEM-F12, Fetal Bovine Serum (FBS), penicillin-streptomycin (10 000 U/mL), nonessential amino acids, insulin transferrin selenium, and Tryple were obtained from (Gibco Invitrogen, Waltham, USA). TGF- β was purchased from (Sigma Aldrich, Minneapolis USA). Human Serum Albumin was purchased from (Irvine Scientific, Santa Ana, USA). SYBR Green PCR Master Mix was acquired from (Ampliqon, Odense, Denmark). Agarose was purchased from (Sina Clon, Tehran, Iran). PCR Master Mix 2X was acquired from (Tac Clon, Tehran, Iran). cDNA Synthesis Kit was purchased from (Yektatajhez, Tehran, Iran) and TRIZOLE was provided from RotiZOL RNA (ROTH, Karlsruhe, Germany). Other chemicals and solvents were of analytical grade and purchased from (Merck Millipore, Darmstadt, Germany).

Fabrication of gelatin-DBM (G/DBM)

Gelatin powder was dissolved in deionized water at 50 °C to yield 6% (w/v) aqueous solution and mixed for 30 minutes at 50 °C until the gelatin solution was completely uniform. Then, DBM was immersed into the gelatin solution, vacuumed for 1 minute to facilitate gelatin penetration into the DBM scaffold pores and shaken for 1 hour at 120 rpm. The composites were gelatinized at 4 °C for 12 hours and lyophilized at -60 °C for 2 days.

Fabrication of chondroitin sulfate-gelatin/DBM(GCS/DBM)

After preparing 6% gelatin solution, CS was added so that

its concentration in the solution was 0.5%. This solution was mixed for 30 minutes at 50 °C to distribute completely the CS in the gelatin. Then, it was prepared like the DBM-gelatin scaffold.

Crosslinking of scaffolds

The porous scaffolds were immersed in the crosslinking solution, containing 20 mM NHS and 50 mM EDC in a solution containing 20% (v/v) of MES buffer 50 mM (pH 5), and 80% (v/v) ethanol and shacked for 24 h at 25 °C. Then, scaffolds were washed thrice with PBS (0.1 M, pH 7.4) and lyophilized for 48 hours at 60 °C.¹⁵

Characterization of the scaffolds

Scanning electron microscopy (SEM)

The SEM method was used to observe the surface and porosity of the scaffolds also the presence and adhesion of cells on the scaffolds. To prepare scaffolds containing cells for SEM analysis, after removing the culture medium and washing the scaffold with a solution (PBS; 0.1 M, pH = 7.4), the cells were fixed with a paraformaldehyde solution (4%) for 2 hours at room temperature (25 °C). In the following, by washing the scaffold with PBS solution (twice), the dehydrating process of the scaffolds with alcohol (in an ethanol series) was done. Finally, the samples were dried overnight in the air. All the scaffolds (cellular or non-cellular) were cut into 1 mm thick pieces with a sharp cutter and then coated with gold (25–30 nm thick) by an automatic coater (20 kV).

Morphological evaluation of the scaffolds

Morphological analysis and the presence or absence of hydroxyapatite on the DBM collagen surface were carried out using Scanning electron microscopy (FE-SEM, Hitachi Japan). Also, Image J software was used to analyze the pore size of scaffolds, and the corresponding histogram was drawn (at least 40 holes were randomly selected for each scaffold).^{15 16}

Swelling ratio of the scaffolds

Scaffolds were weighed in a dry state, immersed in the PBS (pH 7.4), and kept in an incubator at 37 °C. Then, within 72 hour at determined time intervals, scaffolds were removed from the medium, and the excess water of scaffolds was removed with filter paper, and their weight was immediately recorded. The swelling ratio was calculated according to the following equation:

$$\text{Swelling ratio} = 100 \times (WS - WD) / WD$$

Where WS and WD are the weights of the scaffolds at the swelling state and the dry state, respectively.¹⁷

In vitro degradation

Scaffolds (n=3) were immersed in PBS (pH 7.4) and incubated at 37 °C for 48 hours. After equilibration in PBS, samples were weighed using a microbalance (W1) followed by incubation in PBS at 37 °C. At different time intervals, the samples were removed and weighed again

immediately after removing excess water (W2).¹⁰ The degradation ratio of scaffolds was calculated as:

$$\text{Degradation ratio} = 100\% \times (W1 - W2) / W1$$

Mechanical testing

The samples with a diameter of 6 mm and a thickness of 6 mm were prepared in the form of a cylinder, and 1 hour before the analysis, they were immersed in the PBS solution (pH 7.4) at room temperature. The solution was removed, and samples were dried with filter paper.

The compressive modulus of the samples (n=3) was measured using a universal mechanical tester device (Zwick/Z100, Germany). The samples were compressed at a preload of 0.05 N with a 10 N cell ramp speed of 0.5 mm/min until 50% of initial thickness deformation.

The E-modulus of the scaffolds can be calculated by the slope of the compressive stress-strain curve in the deformation of 5%-30% of the samples.^{10,18}

Porosity measurements

Porosity evaluation of scaffolds was performed using the liquid displacement technique. The n-hexane solvent was chosen as the substitution liquid due to its easy permeability in the pores of the scaffolds. DBM, G/DBM, and GCS/DBM scaffolds (with dimensions of 5*5*2 mm) were cut and immersed in a graduated cylinder (15 mL) containing 10 mL of n-hexane solvent (V1) for 30 minutes. The total volume in which the solvent penetrated the holes was noted as V2. After that, the immersed scaffold was removed, and the remaining volume of n-hexane was recorded as V3. The percentage of scaffold porosity was obtained from the following equation¹⁹:

$$\text{Porosity (\%)} = (V1 - V3) / (V2 - V3) * 100$$

Isolation of PMSCs

Fresh placental samples (80 g) were collected from healthy donor mothers after normal delivery at a local hospital with the consent forms observing the ethical principles of Tehran University of Medical Sciences (TUMS) guidelines for human research. Samples were washed 4-5 times with PBS (containing antibiotics) for 1 hour to remove the blood and surgical materials completely. The samples were cut into small pieces with a scalpel blade under sterile conditions and incubated in collagenase IV solution (0.1%) for 3 hours at a 37 °C shaker incubator for enzymatic digestion. Then, using a sterile pipette, the cell suspension was separated from the rest of the undigested tissue and cultured in a culture medium containing DMEM F12, 10% FBS, and penicillin/streptomycin (1X) at 37 °C and 5% CO₂. The medium was changed after 48 hours, and the cells that were not attached were discarded. The third passage of these cells was used for cell studies.²⁰

Characterization of PMSCs

To determine the identity of PMSCs, the expression of

CD90, CD105, CD73, and CD45 markers on the cells was evaluated by flow cytometry.²¹

Cell retention and viability in scaffolds

PMSCs extracted from the human placenta were used to culture the scaffolds in the third passage. PMSCs were detached from the flask with Tryple and Tryple neutralized with a cell culture medium. Then, it was centrifuged, and the cells were counted; the concentration of 3×10^6 cells/ml was re-suspended in a stem cell culture medium. (Cell suspension solution)

After sterilizing the scaffolds in 75% alcohol solution for 4 hours and exposing both sides to UV radiation for 1 h, the scaffolds were immersed in the culture medium overnight to remove the waste materials and remaining alcohol of the scaffolds.

Scaffolds seeded with 3×10^5 PMSCs were then cultured in the medium containing DMEM-F12, 10% FBS 100 units/mL penicillin and 100 µg/mL streptomycin. after 2 and 14 days, samples were removed from the culture medium, washed with PBS and then incubated with the staining solution containing EB and AO with a final concentration of 0.2 µg/mL in PBS at 37 °C for 15 minutes in the dark. Afterward, photography was done by a fluorescence microscope (live and dead cells were stained green and red, respectively).²² Also, the cell retention and proliferation in samples on the 14th day were evaluated with SEM images by staining the nuclei of cells using (1 µg/mL) DAPI after fixing the samples in 4% paraformaldehyde solution. Then, photography was done with a fluorescence microscope.

PMSCs seeding for chondrogenic differentiation

The sterilized DBM, G/DBM, and GCS/DBM scaffolds (According to the method mentioned above) were transferred to a 24-well plate, and 100 µL of the cell suspension solution (about 3×10^5 cells) was slowly transferred onto each scaffold. The scaffolds were incubated for 1 h at 37 °C for attaching the cells to the scaffolds. Then the cartilage differentiation culture medium containing DMEM high glucose (containing 0.11 g/L sodium pyruvate), 1×10^{-7} M dexamethasone, 50 µg / mL L-ascorbic acid 2-phosphate, 1% nonessential amino acids, 1% insulin transferrin and selenium and 10 ng/mL TGF-β1 was added and incubated at 37 °C and 5% CO₂ and the medium was changed every 3 days.^{10,23}

Cartilage-special gene expression analysis

To evaluate the differentiation of PMSCs into cartilage, in the 14th and 21st -time intervals, cultured samples (n=3) in the cartilage differentiation medium, after washing with PBS, were crushed into powder in a mortar free of RNase in the presence of liquid nitrogen, RNA extraction was performed according to the Trizol reagent manufacturer's protocol (Roti[®]ZOL RNA, ROTH). Then, cDNA synthesis was done with the cDNA Synthesis Kit. Finally, real-time PCR quantitative analysis was performed using SYBR Green PCR Master Mix with Applied Biosystems[™] 7500 Real-Time PCR System. Thermal and time profiles for real-time PCR were set as follows: A cycle of 95 °C for 10 minutes followed by 40 cycles (95 °C for 15 seconds, 62 °C for 1 minute). All experiments were run three times. For chondrogenic differentiation, aggrecan (AGC) and collagen 2 (COL-2) genes and for osteogenesis, collagen-1 (COL-1) gene expression were analyzed. The expression levels of the mentioned genes in each scaffold group were normalized to the expression of the housekeeping gene (GAPDH) (calculation of ΔCt), and the relative expression changes of the chondrogenesis and osteogenesis marker genes were calculated using Livak's method $2^{-\Delta\Delta\text{Ct}}$. Changes in $2^{-\Delta\Delta\text{Ct}}$ gene expression were calculated using the following equation: ($\Delta\Delta\text{Ct} = \Delta\text{Ct G/DBM}$ or $\Delta\text{Ct GC/DBM} - \Delta\text{Ct DBM}$).²⁴

Visualization of proteoglycans in scaffolds (Alcian Blue method)

The CS staining method in the scaffold, e.g., GCS/DBM, before cell culture and deposited proteoglycans after cell culture is as follows:

After cultivating PMSCs on all three types of scaffolds at 3×10^5 cells/mL for 21 days in chondrogenic media, the cells were fixed with 4% paraformaldehyde solution on the scaffolds and dehydrated with ethanol series. Then 5 µm slices were prepared, and the sections were stained with the Alcian Blue kit (pH 2.5) overnight, washed with water, and finally stained with nuclear fast red solution (0.1%) for 15-30 minutes. The staining results were recorded using an inverted, light and fluorescent microscope (Olympus, Japan).

Immunostaining evaluation

According to the above method, after fixing, dehydrating, paraffinizing, cutting, deparaffinized, and hydrating with

Table 1. Primer sequences used for RT-qPCR

Gene	Forward primers (5'–3')	Reverse primers (5'–3')	Amplificon (bp)	Tm (°C)	GenBank No.
AGC	TGTCAGATACCCCATCCAC	CATAAAAGACCTCACCTCC	149	55	NM_001135.4
COL-2	GGTCTTGGTGGAACTTTGCT	GGTCCTTGCACTACTCCCAAC	86	59	NM_001844.5
COL-1	TGGAGCAAGAGGCGAGAG	CACCAGCATCACCTTAGC	122	59	NM_000088.4
GAPDH	GGTGAAGGTCGGAGTCAACG	GACAAGCTTCCCGTTCTCAGC	142	61	NM_002046.7

alcohol series and washed with distilled water, scaffolds containing cells were placed in a peroxidase solution for 10 minutes for endogenous peroxidase block process. Then, the antigen retrieval process was performed using an Antigen Retrieval Buffer at a temperature of 95 °C for 10 minutes and incubated for 40 minutes in Master Polymer Plus HRP in the presence of the primary antibody Mouse anti-human Col-2 Monoclonal Antibody. After washing-by-washing buffer, cells were incubated in DAB chromogen solution for 10 minutes at room temperature. after washing with distilled water, they were also incubated in hematoxylin solution for one minute until the nuclei were colored and photographed with an Olympus (Japan) microscope. It was done according to the antibody manufacturer's protocol.

Statistical analysis

Statistical analysis of experimental data was done using GraphPad Prism 9.5.0 software. One-way or two-way analysis of variance (ANOVA) and Tukey's multiple tests were used to compare between groups. For each quantitative analysis, at least 3 repetitions have been done. Quantitative results of analyzes were calculated as mean \pm SEM by the mentioned software, and $P < 0.05$ were introduced as statistically significant.

Results and Discussion

Scaffold fabrication

Totally DBMs were used in the preparation of all scaffolds because the presence of hydroxyapatite crystals on the collagen surface (Fig. 1b) makes it difficult for the collagen surface to be available for the chemical cross-linking reaction and prevents the cross-linking of DBM surface collagen with G or CS molecules, as result scaffold stability

is reduced. (Fig. 1c) shows the complete demineralization and the exposure of the collagen surface. This figure in scale 200 μ m was able to depict only one of the holes of DBM; since the difference in the size of the holes of the DBM scaffold and the modified DBM scaffolds is great, to better show the structure of the scaffolds, the 1mm scale photo was chosen for DBM and 100 μ m for the modified ones (Fig. 1d-f).

To prepare scaffolds, gelatin (G) solution or chondroitin sulfate-gelatin (CSG) was incorporated into the porous structure of DBM, which has relatively large holes. Using a vacuum facilitates the penetration of G solution or CSG inside these cavities by removing the air. Next, by performing gelation, freeze-drying processes, and finally, chemical cross-linking in the presence of EDC and NHS in alcohol solvent (reducing the hydrolysis of gelatin), scaffolds were prepared.²⁵

The function of the porous structure of hydrogels is similar to the extracellular matrix, which, by creating a suitable environment for the permeability of vital nutrients and oxygen to the cells, provides the possibility of cell penetration and proliferation.²⁶

As seen in (Fig. 1a) the DBM scaffold has a gray network structure with visible porosity to the naked eye, and the G/DBM and GCS/DBM scaffolds have a white tablet-like structure with invisible porosity to the naked eye. On the other hand, G penetration in the holes creates a rough surface in G/DBM and GCS/DBM scaffolds, which favors cell adhesion. According to the SEM observation, the size of the G/DBM and GCS/DBM pores was significantly reduced compared to the DBM scaffold. Due to this, gelatin with small pore size filled the large pores of DBM and enhanced the distribution of seeded cells in the modified scaffold (Fig. 1d-f).

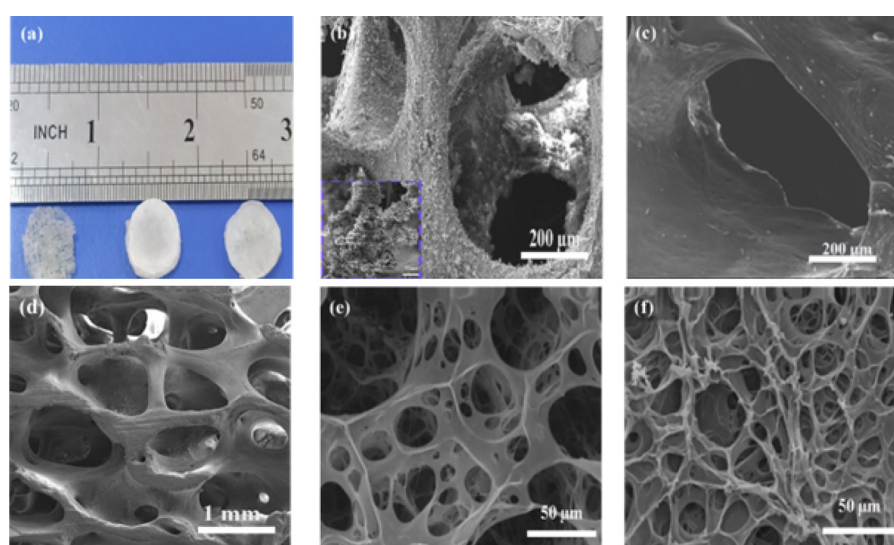


Fig. 1. Gross morphology and scanning electron microscopy of scaffolds. (a) Gross morphology of demineralized bone matrix (DBM), DBM-supported gelatin hydrogel (G/DBM), and DBM-supported chondroitin sulfate-gelatin hydrogel (GCS/DBM), (b) SEM images of the semi-demineralized DBM (hydroxy apatite on the Col-1 surface), (c) SEM images of the completely demineralized DBM (hydroxy apatite free- Col- 1 surface), (d-f) SEM images of the three scaffold groups (d) DBM, (e) G/DBM, (f) GCS/DBM.

Pore size and porosity of scaffolds

SEM images indicate that the pore size of G/DBM and GCS/DBM is significantly reduced than DBM scaffolds. The analysis of the size of the pores using ImageJ software^{15,16} shows that more than 90% of the pore sizes in G/DBM and GCS/DBM scaffolds are smaller than 100 μm , while more than 90% of the pore sizes in DBM are larger than 300 μm (Fig. 2a-c) and this was appropriate for the supply of seeded cells.

After the introduction of gelatin in the cavities of the DBM scaffold, the average porosity decreased significantly (about 7%) and reached 67% in the DBM scaffold to 60% in the hybrid scaffolds. However, hybrid scaffolds still have high porosity (Fig. 2d).

The results of previous research showed that seeding of chondrocytes on the DBM scaffold in cells adhering to the surface, e.g., chondrocytes, due to the large size of the DBM cavities, the interaction of integrin-receptor to the surface decreases. As a result, the tendency of cells to increase cell proliferation and decrease the Production of intercellular matrix changes the phenotype of chondrocytes.⁹

Turnbull et al showed that scaffolds with an average pore diameter of more than 300 μm increased bone formation after implantation due to higher permeability and angiogenic potential, and scaffolds with pores closer to 100 μm are more favorable for cartilage cell growth due to a lack of angiogenic potential within cartilage.^{27,28}

Although the presence of larger pores and more porosity in the scaffold can facilitate the transfer of nutrients and gases (mass transfer) to the cells and the removal of waste materials from them and increase the cell density, it has been observed that the synthesis of cartilage matrix proteins in scaffolds with small pores (about 75 μm) and less porosity is increased. Probably, the reason for this phenomenon is that the small size holes induce adhesion configuration and 3D cell aggregation, and by

reducing cartilage porosity, these factors together can improve the specific synthesis of the extracellular matrix of chondrocytes.²⁹ Therefore, it seems that G-DBM and GC-DBM scaffolds have suitable hole sizes and porosity for use in cartilage tissue reconstruction.

Swelling and degradation

The results of the swelling of the scaffolds showed that all three types of scaffolds gradually swell after absorbing water. Although in the first hour, the swelling rate of gelatin-containing scaffolds is higher than that of DBM scaffolds, it seems that the presence of chemical crosslinks in G/DBM, GC/DBM scaffolds prevents them from swelling further and finally, after 48 h, almost the maximum amount of swelling has occurred (Fig. 3a). The swelling of the three scaffolds was not significantly different from each other.

During the first week, the scaffolds' degradation rate was similar. Still, over time, the rate of degradation of DBM was higher than the other two scaffolds, so that on the 21st day, the percentage of destruction of the DBM scaffold was almost twice that of hybrid scaffolds (G/DBM and GCS/DBM) ($P < 0.0001$). Also, the degradation percentage of the GCS/DBM scaffold was significantly higher than the G/DBM scaffold ($P < 0.005$) (Fig. 3b).

Lai et al reported that since the presence of CS molecules in gelatin hydrogels increases the water absorption power of the scaffold, it is possible to provide more access of the enzyme to the active sites of the gelatin polymer chain and be effective in breaking the peptide bond of the scaffold and it can increase the degradation rate of scaffold.³⁰

Mechanical properties

The results of the mechanical properties test for three types of scaffolds are shown in (Fig. 4). The amount of strain% of the scaffolds compared to the stress (kPa) for all

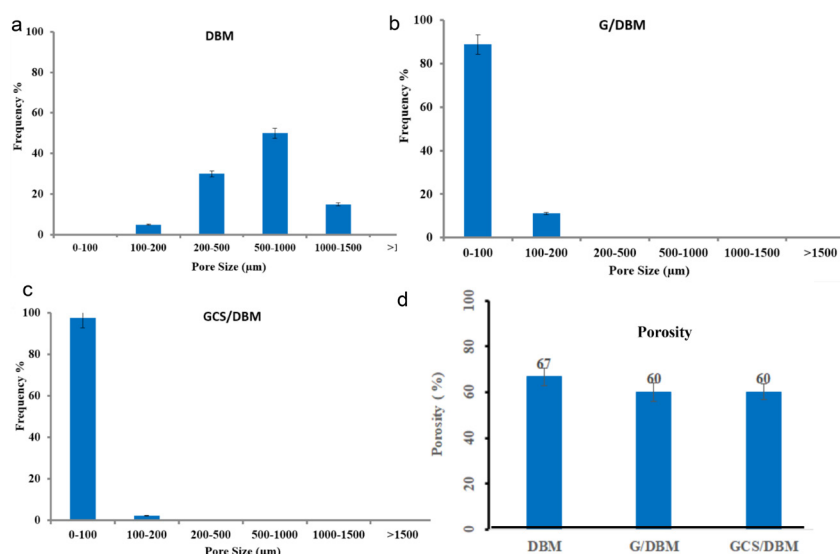


Fig. 2. Histogram of pore size (a, b, c) and porosity (d) of the DBM, G/DBM, GCS/DBM scaffolds.

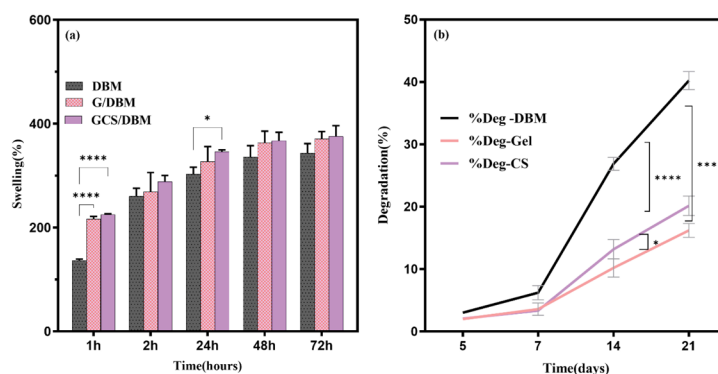


Fig. 3. (a) All three types of scaffolds have high water absorption capacity (>300%), even though the swelling of G/DBM, GCS/DBM hybrid scaffolds in the first hour is significant (**** $P < 0.0001$, * $P < 0.01$, $n = 3$). However, the presence of covalent bonds caused by cross-linking has prevented the swelling of these scaffolds over time. (b) During the first week, there is no significant difference in the rate of destruction of the scaffolds, but on the 21st day, the destruction percentage of the hybrid scaffolds (G/DBM, GCS/DBM) reduced by half (**** $P < 0.0001$, $n = 3$), and the destruction percentage of GCS/DBM was significantly more than G/DBM (* $P < 0.01$, $n = 3$).

three types of scaffolds in the wet state was measured by the Zwick/Z100 device. Then, according to the slope fitting method, by drawing the stress-strain% curve (Fig. 4a), the slope of the first linear range of the curves (% strain) was calculated and reported as compressive mechanical resistance (Fig. 4b).

The results showed that the E-modulus in G/DBM and GCS/DBM scaffolds is extremely (more than 8 times) increased compared to the DBM scaffold (Fig. 4b). Crosslinking and creating covalent bonds improved the mechanical resistance of the scaffolds. These findings are in line with the results of Hoffmann et al, who reported that the crosslinking process is effective in improving the mechanical properties of scaffolds.^{31,32}

Mechanical strength is one of the important characteristics of cartilage tissue, which inherently gives this tissue the ability to perform the relevant function, especially in places that bear high mechanical load.³³ Therefore, in clinical applications, the design of scaffolds with acceptable mechanical properties that can withstand the mechanical loads after grafting the scaffold at the lesion site is one of the key points in the success of cartilage tissue engineering.¹⁰ Also, the mechanical strength of the

scaffolds is one of the effective factors in determining the size of the scaffold holes because, in soft scaffolds with low mechanical strength, the number of contractions and tearing of the scaffolds is more. As a result, cell proliferation is limited. On the contrary, rigid scaffolds maintain their structure and cavity space by resisting cell contractions during cell proliferation and facilitating cell proliferation.¹⁵ It has been reported that the stiff ECM microenvironment can activate the focal adhesion kinase, and as a result, the cell proliferation pathway is activated. So, mechano-transduction pathways can be effective.³³ Furthermore, Provenzano et al showed that the interaction and behavior of chondrocytes, including their cell distribution and mitosis, changes against materials with different hardness of scaffolds is variable.³⁴ Focal adhesions connect the extracellular matrix (ECM) to the intracellular cytoskeleton, which can translate the force between the ECM and the intracellular cytoskeleton into biochemical signals and thus affect cell behavior.³³ The mechanical analysis results of the scaffolds show that the G/DBM and GCS/DBM scaffolds have similar mechanical strength and E-module's of compression, which was not far from expected due to their similar structure (Fig. 4).

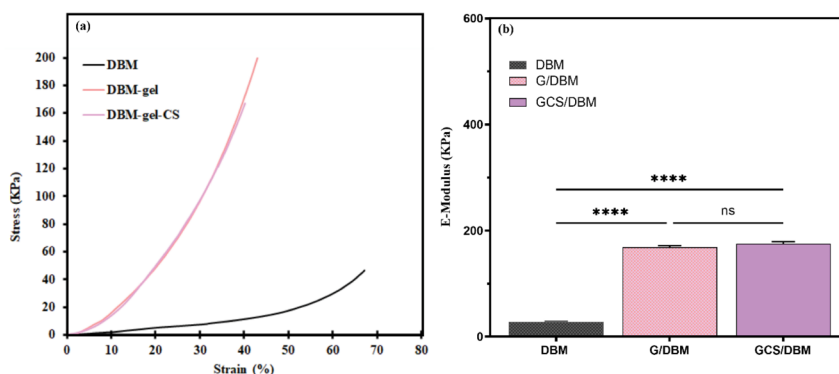


Fig. 4. Mechanical strength of the scaffolds. (a) Stress-strain% curves. (b) E-modulus of the scaffolds was calculated using the slope fitting method in the first linear region of the stress-%-strain curves, and G/DBM, GCS/DBM scaffolds show significantly higher mechanical strength than DBM alone ($n = 3$, **** $P < 0.0001$).

Evaluation of the expression level of specific markers of MSCs

The results of flow cytometry show the high expression of MSCs specific antigens CD90 (100%), CD73 (100%), CD105 (100%), and very low expression of hematopoietic cell antigens, CD45 (0.5%) (Fig. 5).

Cell morphology, attachment, and viability in scaffolds

SEM photos show the morphology of PMSCs on scaffolds containing cells 14 days after cultivation. In these images, PMSCs attached to the surface show stretched-out morphology (Fig. 6), but due to the high density of cells, most of the cells are seen as colonies; AO/EB and DAPI staining photos confirm this issue well (Fig. 7).

Qualitative evaluation of cell attachment and retention on the scaffold was performed by Live-Dead staining (AO-EB); moreover, nuclei of attached cells staining (DAPI), respectively after 2 and 14 days of cell culture (Fig. 7). After 14 days of cell culture, all three types of scaffolds are favorable for the survival and growth of cells and the scaffolds showed no special toxicity.

The rate of adhesion and connection of cells to the scaffold is one of the basic parameters in the success of the scaffold to improve survival and the possibility of proliferation and differentiation of cells on the scaffold. Therefore, optimizing the structure of scaffolds with the help of biomaterials or materials containing cell adhesion motif peptides can achieve this important goal. For example, in scaffolds containing gelatin, cell attachment

and matrix-cell interaction increase due to the presence of RGD peptide (which includes amino acids arginine-glycine-aspartic acid) in the scaffold.^{11,35,36}

In the AO-EB staining images, the light green dots represent living cells two days after cell culturing (the same number of cells). Results showed that, due to the size of the pores and the surface of scaffolds, the number of PMSCs remaining and attached to the scaffolds differed. In the DBM scaffold, more cell escape occurred, and the number of PMSCs attached to the scaffold was less than in modified scaffolds. Also, DAPI staining was done, and the photos clearly show more cell density and distribution of cells on the G/DBM and GCD/DBM scaffolds than on the DBM scaffold (Fig. 7C) which might be because the DBM scaffold with a larger pore size could not hold as many cells as the G/DBM and GC/DBM hybrid scaffolds (Fig. 7A).

The presence of more live PMSCs in G/DBM, GCS/DBM than in DBM scaffolds indicates that modifying the DBM scaffold with G or GCS increases the retention and viability of cells in G/DBM and GCS/DBM compared to the DBM scaffold (Fig. 7B, C).

Evaluation of chondrogenic differentiation of PMSCs by RT-PCR

The difference in chondrogenic differentiation potential of PMSCs on DBM, G/DBM, and GCS/DBM scaffolds was investigated by analyzing the expression levels of chondrogenesis (COL-2, AGC) and dedifferentiation

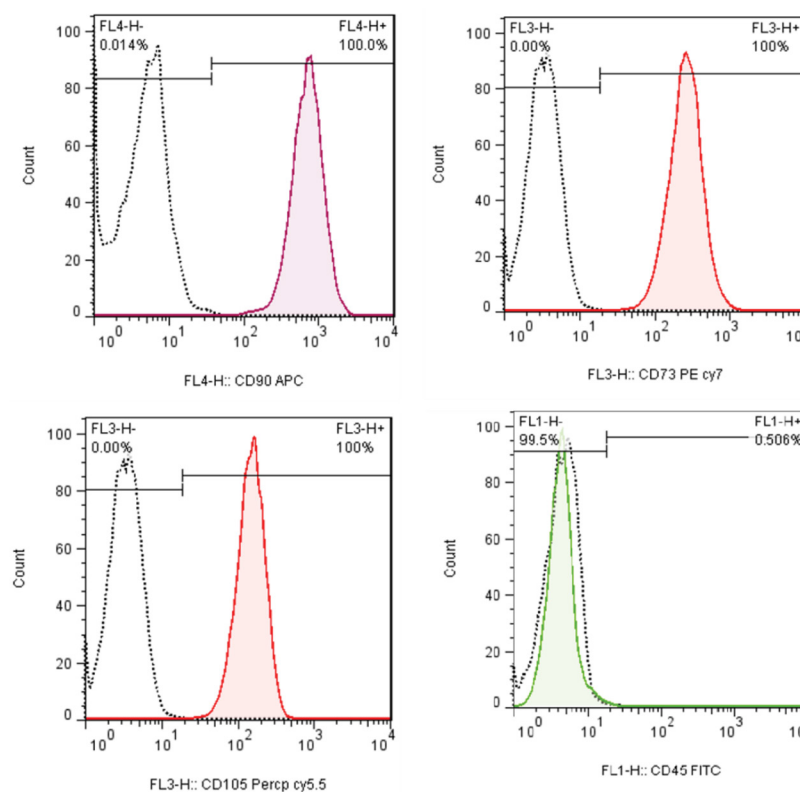


Fig. 5. Evaluation of expression of cell surface-specific markers of MSCs, extracted from placenta tissue.

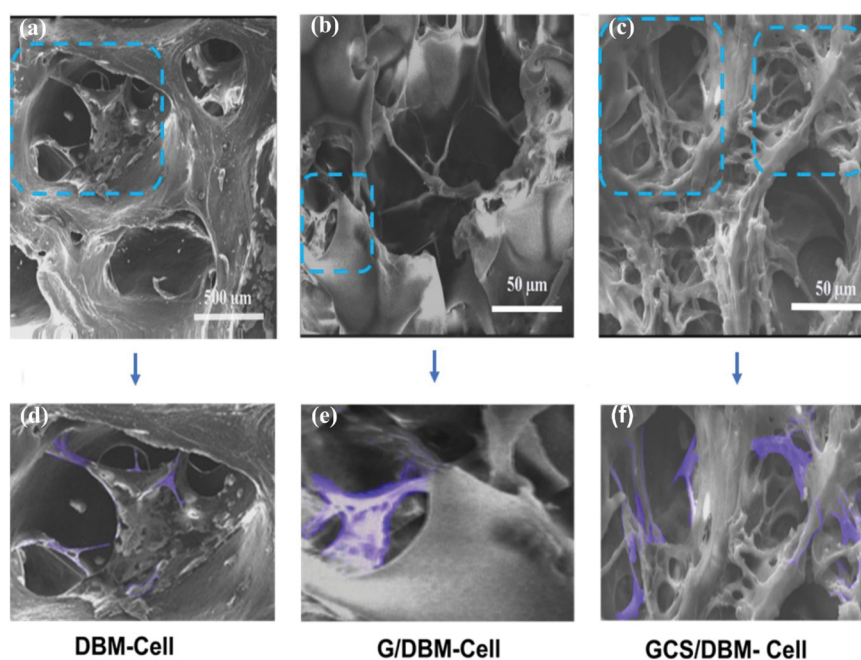


Fig. 6. Morphology and attachment of PMSCs in scaffolds after 14 days of seeding. (a) DBM (b) G/DBM (c) GCS/DBM (The colored areas in (d), (e), and (f) figures respectively show the cells on relevant magnified scaffold).

(COL-1) genes by real-time PCR method.

After 10 and 21 days of cultivation in the chondrogenesis medium, the analysis showed that the expression of AGC in the G/DBM scaffold on days 10 and 21 compared to the DBM scaffold decreased (50%). However, these changes were incremental in the GCS/DBM scaffold, especially on the 21st day, which reached almost 4 times (Fig. 8A-a). Also, the expression of COL-2 in the first 10 days of cultivation for the G/DBM compared to the DBM scaffold

was reached less than half; however, in the GCS/DBM scaffold, increased slightly (about 1.1 times) and by the 21st day, it had doubled (Fig. 8A-b).

The results of Meghdadi et al research show that the CS-grafted polycaprolactone (PCL) scaffolds in a free chondrogenic medium, due to the presence of CS molecules in the scaffold composite, caused an increase in the expression of chondrogenic markers such as Col-2.³⁷ The presence of CS molecules, containing carboxylic acid

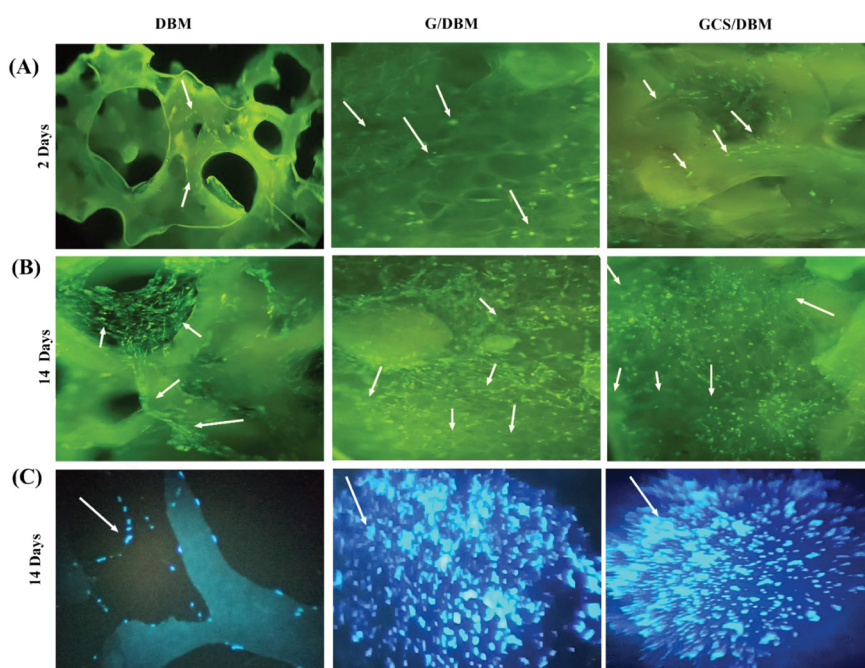


Fig. 7. The staining of PMSCs cultured on the scaffold with EB/AO (A) 2 days after cultivation, (B) 14 days after cultivation (Light green dots indicate living cells), and (C) with DAPI staining 14 days after culture (As the arrows show) light blue points indicate the nucleus of the cells (Magnification: x20).

and sulfate ester groups, creates polar molecules with a high negative charge in the scaffold, which can effectively absorb growth factors with a positive charge and ultimately stimulate differentiation towards chondrogenesis.³⁸ Similarly, the studies of Tamaddon et al showed that the presence of unbound CS in hydrogel can also provide a suitable environment for the chondrogenic differentiation of MSCs.³⁹ Therefore, according to the previous studies, the presence of CS in the GCS/DBM scaffold has made the conditions more favorable for the expression of COL-2 and AGC. So, the expression of AGC and COL-2 increased with the enhancement of scaffold degradation and CS release.

The expression of COL-1 in the first 10 days for G/DBM and GCS/DBM scaffolds compared to DBM has reached less than half, but in the G/DBM scaffold, it has increased by 1.4 times until day 21; For the GCS/DBM scaffold, it was not significantly different from DBM (Fig. 8A-c). It has been reported that scaffolds with an average hole size of 300 μm are more suitable for osteogenesis, and

scaffolds with a hole size of 100 μm are more suitable for chondrogenesis.⁴⁰ Based on this finding, it can probably be said that in the early days of cell culture, the extent of scaffold destruction was insignificant. More than 90% of the holes were smaller than 100 nm and the conditions were unsuitable for bone differentiation. Gradually, with the increase in scaffold destruction and the size of the holes, the conditions for osteogenesis and COL-1 expression have become more favorable.

Evaluation of proteoglycans in scaffolds

The evaluation of the difference in the potential of the scaffolds in supporting the production and secretion of proteoglycans and sGAG was done by Alcian Blue staining of the scaffolds (Fig. 8B-a, b). This staining shows existing or secreted proteoglycans and sGAG in blue. In the staining of cell-free scaffolds, the presence of scattered blue dots in the GCS/DBM scaffold and the absence of these blue dots in the two groups of DBM and G/DBM scaffolds completely confirms the presence of

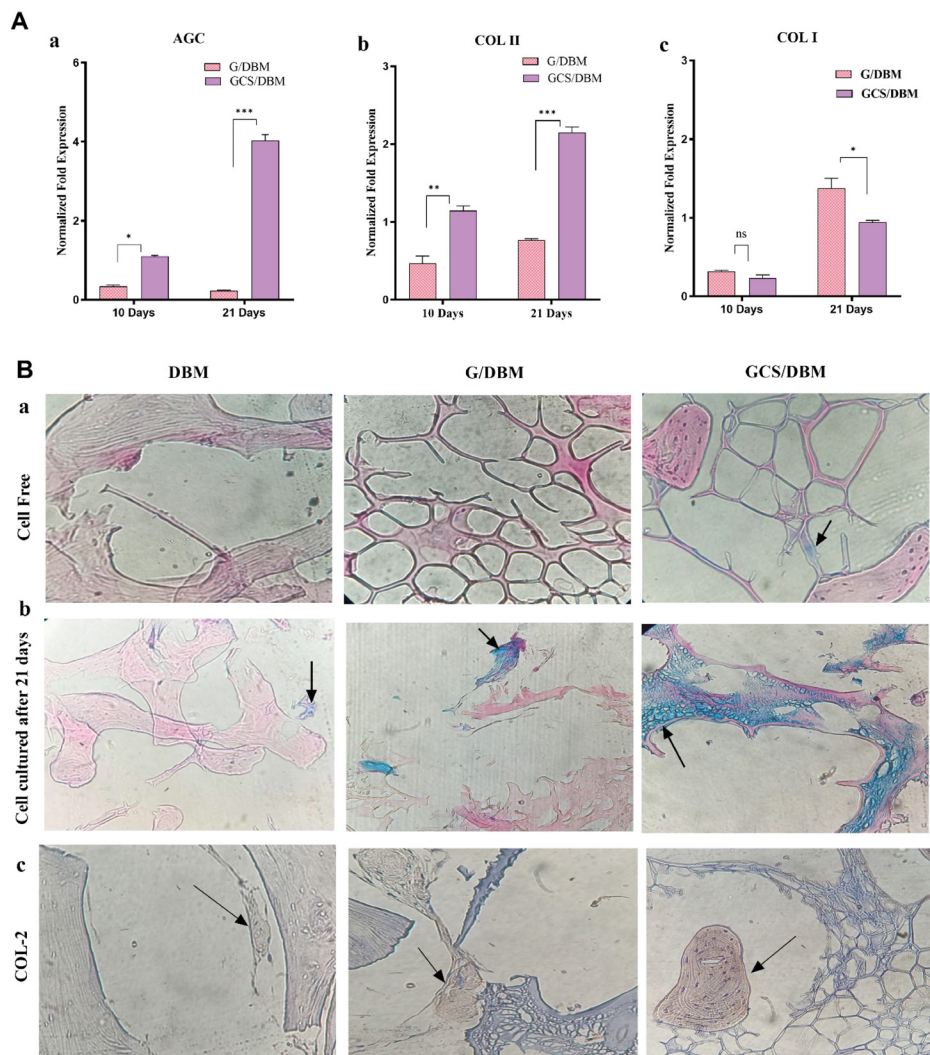


Fig. 8. A. Quantitative gene expression analysis of the cartilage-specific genes a) AGC, b) COL-2, and osteogenesis gen c) COL-1 (n=3, *P<0.05, **P<0.01, ***P<0.001) within the G/DBM, GCS/DBM scaffolds after 10 and 21 days of in vitro culture. The G/DBM and GCS/DBM gene expression levels were normalized to DBM.

Research Highlights

What is the current knowledge?

√ DBM scaffold is widely used in bone and cartilage tissue engineering due to its biocompatibility and biodegradability.
 √ Fabricated scaffolds based on DBM for cartilage tissue engineering mostly include β -glycerophosphate chitosan, which showed low stability and mechanical resistance due to ionic physical crosslinking.

What is new here?

√ The GCS/DBM scaffold was fabricated in the presence of an EDC-NHS (chemical crosslinker), and analysis results showed that the stability and mechanical strength of this scaffold was greatly improved (more than 8-fold).
 √ CS in the GCS/DBM scaffold improved the expression of chondrogenic key markers such as COL-2 (about 2.2-fold) and GAGs (about 4-fold), rather than G/DBM and DBM scaffold.

CS in the GCS/DBM scaffold (Fig. 8B-a). The staining of the scaffolds containing PMSCs that were cultured for 21 days in the cartilage differentiation medium showed that the secretion of proteoglycans and sGAG occurred at a low rate in the DBM and G/DBM scaffolds. However, in the GCS/DBM scaffold, high secretion of proteoglycans and sGAG can be seen in an integrated and uniform manner in the matrix around the cells. These findings are completely consistent with real-time PCR gene expression data. It confirms that the presence of biomaterials is similar to the natural cartilage tissue in cartilage tissue engineering scaffolds. It supports cartilage differentiation and especially increases the expression of their similar component. Similar results have been reported in another research.^{41,42}

Immunostaining evaluation

Type 2 collagen is a special component produced by cells during cartilage differentiation. After 21 days of cell culture in cartilage differentiation medium on the scaffolds, it shows that the cells grown on the GCS/DBM scaffold, compared to the cells cultured on the G/DBM scaffold, have more amounts of COL-2 in a denser form and produced more integrated. However, the collagen produced in the DBM scaffold was only very partial. Type 2 collagen can be seen in brown color in the images, and cell nuclei in blue (Fig. 8B-c). These results are consistent with the results of real-time PCR analysis.

The effect of CS in scaffolds on the synthesis of more COL-2 in the extracellular matrix has been reported many times. So, even in the conditions where the culture medium lacked growth factors, it helped to increase the expression and secretion of COL-2.^{41,43}

Conclusion

This study investigated the differences in biophysical,

biomechanical capabilities, and chondrogenic differentiation potential of PMSCs on DBM-based scaffolds modified with gelatin or gelatin-chondroitin sulfate chemical crosslinks. Although type 1 collagen-based scaffolds have insufficient cartilage differentiation compared to type 2, however the arthritogenic potential of type 2 collagen has limited its clinical use.⁴³

Since the ultimate goal of tissue engineering research is the clinical applications of the projects, we applied the DBM as a foundation scaffold, which is naturally made of COL-1 and has physical properties such as inherent 3D-biomaterial structure, porosity, mechanical resistance, and swelling ability. Optimizing the size of the holes leads to the reduction of cell escape; by introducing gelatin into the holes, the size of the holes is reduced, and the surface of the scaffold increases. On the other hand, by taking advantage of the presence of the RGD group in the gelatin structure, cell retention and attachment of the scaffold can be improved. Also, with chemical crosslinking, the mechanical strength of the scaffold significantly increased, which is one of the important parameters in the scaffolds used in cartilage regeneration. Using CS biomaterial, which is also present in the natural structure of cartilage, the expression of COL-2 and especially AGC has been upgraded, and the cartilage differentiation of PMSCs has been improved compared to the DBM scaffold. Therefore, the GCS/DBM scaffold seems promising for differentiating placental mesenchyme stem cells for cartilage tissue engineering.

Acknowledgments

The authors gratefully thank the Molecular Research Center of Genesaze Co., on sharing their knowledge and equipment for this work.

Authors' Contribution

Conceptualization: Fatemeh Haghwerdi, Ismaeil Haririan, Masoud Soleimani.

Data curation: Ismaeil Haririan, Masoud Soleimani.

Formal analysis: Masoud Soleimani.

Funding acquisition: Ismaeil Haririan.

Investigation: Fatemeh Haghwerdi.

Methodology: Fatemeh Haghwerdi, Ismaeil Haririan, Masoud Soleimani.

Project administration: Ismaeil Haririan, Masoud Soleimani.

Resources: Fatemeh Haghwerdi, Masoud Soleimani.

Software: Fatemeh Haghwerdi.

Supervision: Ismaeil Haririan.

Validation: Ismaeil Haririan, Masoud Soleimani.

Visualization: Masoud Soleimani.

Writing—original draft: Fatemeh Haghwerdi

Writing—review & editing: Ismaeil Haririan, Masoud Soleimani.

Competing interests

There are no conflicts of interest.

Ethical Statement

This study was approved by the Ethics Committee of Tehran University of Medical Sciences (IR.TUMS.PSRC.REC.1396.3705).

Funding

This work was part of a Ph.D. thesis and was financially supported by the Tehran University of Medical Sciences, Tehran, Iran (grant No. 9321472002).

References

- Buckwalter JA, Mankin HJ, Grodzinsky AJ. Articular cartilage and osteoarthritis. *Instructional Course Lectures-American Academy of Orthopaedic Surgeons* **2005**; 54: 465.
- Sophia Fox AJ, Bedi A, Rodeo SA. The basic science of articular cartilage: structure, composition, and function. *Sports Health* **2009**; 1: 461-8. <https://doi.org/10.1177/1941738109350438>
- Osteoarthritis (OA). CDC website. Available from: <https://www.cdc.gov/arthritis/basics/osteoarthritis.htm>.
- Hunter DJ, Schofield D, Callander E. The individual and socioeconomic impact of osteoarthritis. *Nat Rev Rheumatol* **2014**; 10: 437-41. <https://doi.org/10.1038/nrrheum.2014.44>
- Cui A, Li H, Wang D, Zhong J, Chen Y, Lu H. Global, regional prevalence, incidence and risk factors of knee osteoarthritis in population-based studies. *EClinicalMedicine* **2020**; 29-30: 100587. <https://doi.org/10.1016/j.eclinm.2020.100587>
- Everhart JS, Jiang EX, Poland SG, Du A, Flanigan DC. Failures, Reoperations, and Improvement in Knee Symptoms Following Matrix-Assisted Autologous Chondrocyte Transplantation: A Meta-Analysis of Prospective Comparative Trials. *Cartilage* **2021**; 13: 1022S-35S. <https://doi.org/10.1177/1947603519870861>
- Huey DJ, Hu JC, Athanasios KA. Unlike bone, cartilage regeneration remains elusive. *Science* **2012**; 338: 917-21. <https://doi.org/10.1126/science.1222454>
- Chen Y, Xu W, Shafiq M, Song D, Xie X, Yuan Z, et al. Chondroitin sulfate cross-linked three-dimensional tailored electrospun scaffolds for cartilage regeneration. *Biomater Adv* **2022**; 134: 112643. <https://doi.org/10.1016/j.jmsec.2022.112643>
- Liese J, Marzahn U, El Sayed K, Pruss A, Haisch A, Stoelzel K. Cartilage tissue engineering of nasal septal chondrocyte-macrophage aggregates in human demineralized bone matrix. *Cell Tissue Bank* **2013**; 14: 255-66. <https://doi.org/10.1007/s10561-012-9322-4>
- Huang H, Zhang X, Hu X, Dai L, Zhu J, Man Z, et al. Directing chondrogenic differentiation of mesenchymal stem cells with a solid-supported chitosan thermogel for cartilage tissue engineering. *Biomater* **2014**; 9: 035008. <https://doi.org/10.1088/1748-6041/9/3/035008>
- Huang H, Zhang X, Hu X, Shao Z, Zhu J, Dai L, et al. A functional biphasic biomaterial homing mesenchymal stem cells for in vivo cartilage regeneration. *Biomaterials* **2014**; 35: 9608-19. <https://doi.org/10.1016/j.biomaterials.2014.08.020>
- Haghwerdi F, Ravari MK, Taghiyar L, Shamekhi MA, Jahangir S, Haririan I, et al. Application of bone and cartilage extracellular matrices in articular cartilage regeneration. *Biomed Mater* **2021**; 16: 042014. <https://doi.org/10.1088/1748-605X/ac094b>
- Meng Q, Man Z, Dai L, Huang H, Zhang X, Hu X, et al. A composite scaffold of MSC affinity peptide-modified demineralized bone matrix particles and chitosan hydrogel for cartilage regeneration. *Sci Rep* **2015**; 5: 17802. <https://doi.org/10.1038/srep17802>
- Corradetti B, Taraballi F, Minardi S, Van Eps J, Cabrera F, Francis LW, et al. Chondroitin sulfate immobilized on a biomimetic scaffold modulates inflammation while driving chondrogenesis. *Stem Cells Transl Med* **2016**; 5: 670-82. <https://doi.org/10.5966/sctm.2015-0233i>
- Chen S, Zhang Q, Nakamoto T, Kawazoe N, Chen G. Gelatin scaffolds with controlled pore structure and mechanical property for cartilage tissue engineering. *Tissue Eng Part C Methods* **2016**; 22: 189-98. <https://doi.org/10.1089/ten.tec.2015.0281>
- Di Luca A, Szlazak K, Lorenzo-Moldero I, Ghebes CA, Lepedda A, Swieszkowski W, et al. Influencing chondrogenic differentiation of human mesenchymal stromal cells in scaffolds displaying a structural gradient in pore size. *Acta Biomaterialia* **2016**; 36: 210-9. <https://doi.org/10.1016/j.actbio.2016.03.014>
- Felfel RM, Gideon-Adeniyi MJ, Zakir Hossain KM, Roberts GAF, Grant DM. Structural, mechanical and swelling characteristics of 3D scaffolds from chitosan-agarose blends. *Carbohydr Polym* **2019**; 204: 59-67. <https://doi.org/10.1016/j.carbpol.2018.10.002>
- Thitiset T, Damrongsakkul S, Yodmuang S, Leeanansaksiri W, Apinun J, Honsawek S. A novel gelatin/chitoooligosaccharide/demineralized bone matrix composite scaffold and periosteum-derived mesenchymal stem cells for bone tissue engineering. *Biomater Res* **2021**; 25: 19. <https://doi.org/10.1186/s40824-021-00220-y>
- Wang SJ, Jiang D, Zhang ZZ, Huang AB, Qi YS, Wang HJ, et al. Chondrogenic Potential of Peripheral Blood Derived Mesenchymal Stem Cells Seeded on Demineralized Cancellous Bone Scaffolds. *Sci Rep* **2016**; 6: 36400. <https://doi.org/10.1038/srep36400>
- Kamalabadi-Farahani M, Vasei M, Ahmadbeigi N, Ebrahimi-Barough S, Soleimani M, Roozafzoon R. Anti-tumour effects of TRAIL-expressing human placental derived mesenchymal stem cells with curcumin-loaded chitosan nanoparticles in a mice model of triple negative breast cancer. *Artif Cells Nanomed Biotechnol* **2018**; 46: S1011-S21. <https://doi.org/10.1080/21691401.2018.1527345>
- Heirani-Tabasi A, Toosi S, Mirahmadi M, Mishan MA, Bidkhorri HR, Bahrami AR, et al. Chemokine Receptors Expression in MSCs: Comparative Analysis in Different Sources and Passages. *Tissue Eng Regen Med* **2017**; 14: 605-15. <https://doi.org/10.1007/s13770-017-0069-7>
- Dadgar N, Ghiaseddin A, Irani S, Tafti SHA, Soufi-Zomorrod M, Soleimani M. Bioartificial injectable cartilage implants from demineralized bone matrix/PVA and related studies in rabbit animal model. *J Biomater Appl* **2021**; 35: 1315-26. <https://doi.org/10.1177/0885328220976552>
- Safari F, Fani N, Eglin D, Alini M, Stoddart MJ, Baghaban Eslaminejad M. Human umbilical cord-derived scaffolds for cartilage tissue engineering. *J Biomed Mater Res A* **2019**; 107: 1793-802. <https://doi.org/10.1002/jbm.a.36698>
- Vassallo V, Tsianaka A, Alessio N, Grubel J, Cammarota M, Tovar GEM, et al. Evaluation of novel biomaterials for cartilage regeneration based on gelatin methacryloyl interpenetrated with extractive chondroitin sulfate or unsulfated biotechnological chondroitin. *J Biomed Mater Res A* **2022**; 110: 1210-23. <https://doi.org/10.1002/jbm.a.37364>
- Ghassemi Z, Slaughter G, editors. Cross-linked electrospun gelatin nanofibers for cell-based assays. 2018 40th Annual International Conference of the IEEE Engineering in Medicine and Biology Society (EMBC); 18-21 July **2018**: Honolulu, HI, USA.
- Lee SH, Shim KY, Kim B, Sung JH. Hydrogel-based three-dimensional cell culture for organ-on-a-chip applications. *Biotechnology Progress* **2017**; 33: 580-9. <https://doi.org/10.1002/btpr.2457>
- Turnbull G, Clarke J, Picard F, Riches P, Jia L, Han F, et al. 3D bioactive composite scaffolds for bone tissue engineering. *Bioact Mater* **2018**; 3: 278-314. <https://doi.org/10.1016/j.bioactmat.2017.10.001>
- Zeltinger J, Sherwood JK, Graham DA, Mueller R, Griffith LG. Effect of pore size and void fraction on cellular adhesion, proliferation, and matrix deposition. *Tissue Eng* **2001**; 7: 557-72. <https://doi.org/10.1089/107632701753213183>
- Nava MM, Draghi L, Giordano C, Pietrabissa R. The effect of scaffold pore size in cartilage tissue engineering. *J Appl Biomater Funct Mater* **2016**; 14: e223-9. <https://doi.org/10.5301/jabfm.5000302>
- Lai JY, Li YT, Cho CH, Yu TC. Nanoscale modification of porous gelatin scaffolds with chondroitin sulfate for corneal stromal tissue engineering. *Int J Nanomedicine* **2012**; 7: 1101-14. <https://doi.org/10.2147/IJN.S28753>
- Lim DJ. Cross-Linking Agents for Electrospinning-Based Bone Tissue Engineering. *Int J Mol Sci* **2022**; 23: 5444. <https://doi.org/10.3390/ijms23105444>
- Hoffmann B, Seitz D, Mencke A, Kokott A, Ziegler G. Glutaraldehyde and oxidised dextran as crosslinker reagents for chitosan-based scaffolds for cartilage tissue engineering. *J Mater Sci Mater Med* **2009**; 20: 1495-503. <https://doi.org/10.1007/s10856-009-3707-3>
- Provenzano PP, Keely PJ. Mechanical signaling through the cytoskeleton regulates cell proliferation by coordinated focal

- adhesion and Rho GTPase signaling. *J Cell Sci* **2011**; 124: 1195-205. <https://doi.org/10.1242/jcs.067009>
34. Haugh MG, Murphy CM, McKiernan RC, Altenbuchner C, O'Brien FJ. Crosslinking and mechanical properties significantly influence cell attachment, proliferation, and migration within collagen glycosaminoglycan scaffolds. *Tissue Engineering Part A* **2011**; 17: 1201-8. <https://doi.org/10.1089/ten.tea.2010.0590>
 35. Huang CY, Hu KH, Wei ZH. Comparison of cell behavior on pva/pva-gelatin electrospun nanofibers with random and aligned configuration. *Sci Rep* **2016**; 6: 37960. <https://doi.org/10.1038/srep37960>
 36. Dutta SD, Hexiu J, Patel DK, Ganguly K, Lim K-T. 3D-printed bioactive and biodegradable hydrogel scaffolds of alginate/gelatin/cellulose nanocrystals for tissue engineering. *Int J Biol Macromol* **2021**; 167: 644-58. <https://doi.org/10.1016/j.ijbiomac.2020.12.011>
 37. Meghdadi M, Pezeshki-Modaress M, Irani S, Atyabi SM, Zandi M. Chondroitin sulfate immobilized PCL nanofibers enhance chondrogenic differentiation of mesenchymal stem cells. *Int J Biol Macromol* **2019**; 136: 616-24. <https://doi.org/10.1016/j.ijbiomac.2019.06.061>
 38. Sorrell JM, Somoza RA, Caplan AI. Human mesenchymal stem cells induced to differentiate as chondrocytes follow a biphasic pattern of extracellular matrix production. *J Orthop Res* **2018**; 36: 1757-66.
 39. Tamaddon M, Burrows M, Ferreira S, Dazzi F, Apperley J, Bradshaw A, et al. Monomeric, porous type II collagen scaffolds promote chondrogenic differentiation of human bone marrow mesenchymal stem cells in vitro. *Sci Rep* **2017**; 7: 43519. <https://doi.org/10.1038/srep43519>
 40. Haung SM, Lin YT, Liu SM, Chen JC, Chen WC. In Vitro Evaluation of a Composite Gelatin-Hyaluronic Acid-Alginate Porous Scaffold with Different Pore Distributions for Cartilage Regeneration. *Gels* **2021**; 7: 165. <https://doi.org/10.3390/gels7040165>
 41. Sechriest VE, Miao YJ, Niyibizi C, Westerhausen-Larson A, Matthew HW, Evans CH, et al. GAG-augmented polysaccharide hydrogel: a novel biocompatible and biodegradable material to support chondrogenesis. *J Biomed Mater Res* **2000**; 49: 534-41. [https://doi.org/10.1002/\(sici\)1097-4636\(20000315\)49:4<534::aid-jbm12>3.0.co;2-#](https://doi.org/10.1002/(sici)1097-4636(20000315)49:4<534::aid-jbm12>3.0.co;2-#)
 42. Sechriest VE, Miao YJ, Niyibizi C, Westerhausen-Larson A, Matthew HW, Evans CH, et al. GAG-augmented polysaccharide hydrogel: A novel biocompatible and biodegradable material to support chondrogenesis. *Journal of Biomedical J Biomed Mater Res* **2000**; 49: 534-41. [https://doi.org/10.1002/\(SICI\)1097-4636\(20000315\)49:4<534::AID-JBM12>3.0.CO;2-%23](https://doi.org/10.1002/(SICI)1097-4636(20000315)49:4<534::AID-JBM12>3.0.CO;2-%23)
 43. Irawan V, Sung T-C, Higuchi A, Ikoma T. Collagen scaffolds in cartilage tissue engineering and relevant approaches for future development. *Tissue Eng Regen Med* **2018**; 15: 673-97. <https://doi.org/10.1007/s13770-018-0135-9>